

Effects of geometry on linear and non-linear gyrokinetic simulations, and development of a global version of the GENE code

X. Lapillonne*, T. Dannert*, S. Brunner*, A. Marinoni*, S. Jolliet*,
L. Villard*, F. Jenko[†], T. Goerler[†] and F. Merz[†]

**Ecole Polytechnique Fédérale de Lausanne (EPFL),
Centre de Recherches en Physique des Plasmas,*

Association Euratom-Confédération Suisse, CH-1015 Lausanne, Switzerland

[†]Max-Planck-Institut für Plasmaphysik, Boltzmannstr. 2, D-85748 Garching, Germany

Abstract. Using an interface with the ideal MHD equilibrium code CHEASE, numerical simulations are performed in realistic Tokamak geometry with the gyrokinetic flux tube code GENE [1, 2]. As a starting point in view of a more general study of geometrical effects on various types of microturbulence, elongation and triangularity scans are carried out in the ITG regime. In particular, the main dependence of the linear growth rate on elongation is identified to result from the modification of the spatial profile gradients. Non-linear simulations have also been performed, and the influence of geometry on the Dimits shift [3] has been investigated.

In order to address the issue of non-local effects in turbulent transport, some of the standard flux tube assumptions are being released in the GENE code, which will thus be extended to allow for radial variations of the equilibrium quantities. The current state of this code development is presented.

INTRODUCTION

There is a growing interest in studying the effect of plasma shaping on microturbulence by means of gyrokinetic codes. Some earlier studies suggested a stabilizing effect of elongation on ITG modes and Trapped Electron Modes and a smaller effect of triangularity [4, 5, 6]. In order to address this issue in tokamak devices, the gyrokinetic flux tube code GENE [1, 2] is used in combination with an interface to the MHD equilibrium code CHEASE. In view of validating this interface, comparisons have been carried out between simulations using the standard $s - \alpha$ equilibrium model and a circular MHD equilibrium for Cyclone base case parameters. Significant differences are found, which are explained by the approximation made in the standard $s - \alpha$ implementation between the straight field line angle and the geometrical poloidal angle, leading to inconsistencies of order $\varepsilon = r/R$. The interface with the equilibrium code is then used to effectuate a scan in elongation κ and triangularity δ in the ITG regime. However, it turns out that there is not a unique way to perform such scans, and the question arises of which quantities to keep constant while changing κ and δ . For example, when going from a concentric circular equilibrium to a situation with elongation and triangularity, the temperature gradient, which was at first constant on a given flux surface, becomes a function of the poloidal angle in the latter case. One could then for instance either choose to keep

the gradient on the equatorial mid-plane constant or keep the effective gradient, such as its flux-surface averaged value, constant while changing the geometrical parameters of the plasma. In this work, we present a specific methodology for such parameter scans, and in particular the issue of the temperature gradient is addressed.

Large scale effects of microturbulence are beyond the scope of the current GENE code, which uses a standard flux tube representation assuming $\rho^* = \rho_s/a \rightarrow 0$, with a the minor radius and ρ_s the ion sound Larmor radius. In order to study non-local effects in turbulent transport, a global version of the GENE code is under development. As a first step towards this goal, the x variation of equilibrium quantities will be introduced, which requires to replace the original Fourier representation for the radial direction by a real space treatment. The current stage of this modification is exposed.

GYROKINETIC EQUATION FOR GENERAL AXISYMMETRIC EQUILIBRIUM

We consider the (x, y, z) field aligned coordinates, where x is a radial coordinate, y the binormal coordinate, and z a parallel coordinate. The following equations are given considering electrostatic modes only and assuming adiabatic electronic response and low β plasma. The code solves the gyrokinetic equation for the particle distribution function $f(t, x, y, z, v_{\parallel}, \mu) = f_0 + f_1$:

$$-\frac{\partial f_1}{\partial t} = \left[\frac{1}{L_n} + \frac{1}{L_T} (v_{\parallel}^2 + \mu B - 3/2) \right] f_0 \frac{\partial \bar{\Phi}_1}{\partial y} + \left[\frac{\partial \bar{\Phi}_1}{\partial x} \frac{\partial f_1}{\partial y} - \frac{\partial \bar{\Phi}_1}{\partial y} \frac{\partial f_1}{\partial x} \right] + \frac{1}{B} \frac{\mu B + 2v_{\parallel}^2}{\sigma} (K_x \mathcal{G}_x + K_y \mathcal{G}_y) + \alpha \frac{v_{\parallel}}{JB} \mathcal{G}_z - \frac{\mu \alpha}{2JB} \frac{\partial f_1}{\partial v_{\parallel}} \frac{\partial B}{\partial z},$$

where $1/L_{Ti} = -d \ln T_i / dx$, $1/L_n = -d \ln n / dx$, $\mathcal{G}_j = \partial_j f_1 + (\sigma_i / v_{\parallel}) \partial_j \bar{\Phi}_1 \partial f_0 / \partial v_{\parallel}$ for $j = (x, y, z)$, $\alpha_i = v_{Ti} / c_s$, $\sigma_i = Z_i T_e / T_i$, $\bar{\Phi}_1$ is the gyroaveraged electrostatic potential, (K_x, K_y) are geometrical coefficients, and $J = [(\nabla x \times \nabla y) \cdot \nabla z]^{-1}$ is the Jacobian .

The self-consistent electrostatic field is solved using the gyrokinetic quasi-neutrality equation :

$$Z^2 \tau [1 - \Gamma_0(b)] \Phi_1 = \pi Z B \int J_0(\lambda) f_1 dv_{\parallel} d\mu - (\Phi_1 - \langle \Phi_1 \rangle), \quad (1)$$

with $b = 1/(\tau B^2) \nabla_{\perp}^2$, $\lambda^2 = 2\mu / B \nabla_{\perp}^2$, and $\langle \rangle$ stands for the flux-surface averaging. The different equilibrium quantities are provided via an interface with the MHD equilibrium code CHEASE [7].

CYCLONE TEST CASE

In order to validate the interface with the equilibrium code, simulations are performed for Cyclone like parameters, namely $q = 1.42$, $\hat{s} = (\rho/q) dq/d\rho = 0.8$, and $\varepsilon = r/R = 0.18$. Here the radial variable is defined as $\rho = \sqrt{\Phi/\Phi_e}$, Φ is the toroidal flux, and Φ_e its value at the edge. The gradient values are defined as $R \langle \nabla \ln T_i \rangle = 6.96$, $R \langle \nabla \ln n \rangle =$

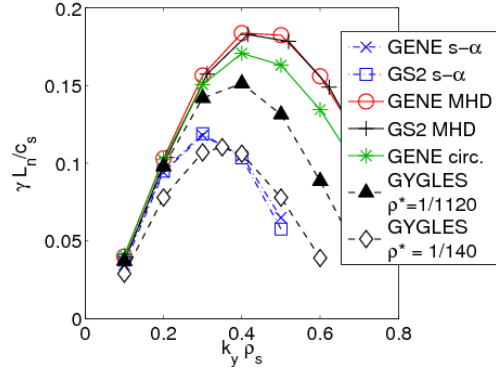


FIGURE 1. Growth rate spectra of linear ITG modes in the Cyclone test case using flux-tube codes with different equilibrium models: MHD (circles: GENE; +: GS2), $s - \alpha$ (crosses: GENE; squares: GS2), and ad-hoc circular concentric (stars: GENE). Results using the global code GYGLES using the ad-hoc circular concentric model are also shown for $\rho^* = 1/140$ (diamonds) and $\rho^* = 1/1120$ (triangles).

2.23. A significant difference is found, see Fig. 1, in the linear growth rates of ITG modes between simulations using the standard $s - \alpha$ model and those using an MHD equilibrium. Such results are confirmed by the GS2 code [8, 9] which was run either with the $s - \alpha$ equilibrium model or with the same MHD equilibrium. In the standard implementation of the $s - \alpha$ model, the straight field line poloidal angle is approximated to the geometric poloidal angle. Such an approximation leads to inconsistencies of order $\varepsilon = r/R$, which have been identified as the source for the observed differences. Agreement within 10% with MHD equilibrium results is indeed reached when using a circular concentric flux surface equilibrium model which correctly treats the straight field line angle.

Having in mind that global simulations are expected to approach flux tube results for $\rho^* \rightarrow 0$, the previous simulations are compared with results from the global code GYGLES, for different values of ρ^* . For larger values of ρ^* ($1/\rho^* = 140$), it turns out that these global results are comparable to the flux tube simulations using the faulty $s - \alpha$ equilibrium model. However, this apparent match, which has been previously reported in [3], is in fact purely coincidental and true agreement is obtained between global results in the appropriate limit $\rho^* \rightarrow 0$ ($1/\rho^* = 1120$) and flux tube simulations with correct magnetic equilibrium treatment.

ELONGATION AND TRIANGULARITY SCAN

The methodology chosen for these parameter scans is the following : equilibria are computed with fixed value of $q = 1.42$ and $\hat{s} = \rho/qdq/d\rho = 0.8$ at the reference flux surface $\rho = 0.5$ by adapting the current profile, while elongation κ and triangularity δ are modified for the Last Closed Flux Surface (LCFS). In addition, the aspect ratio at the LCFS is kept constant. Simulations are then carried out for each equilibrium with the density gradient set to zero ($|\nabla \ln N| = 0$) and for various values of the temperature gradient.

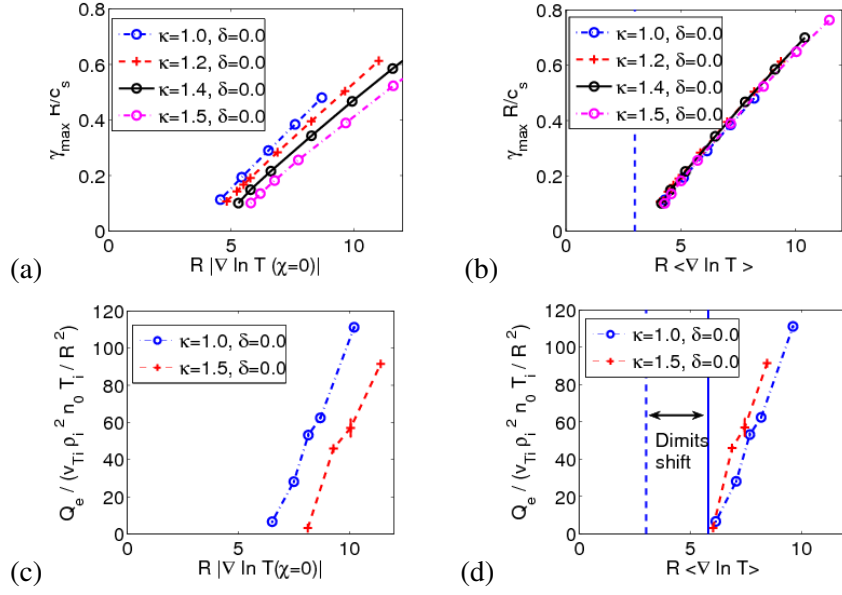


FIGURE 2. Elongation scan at constant triangularity : (a,b) linear growth rate, (c,d) nonlinear electrostatic heat flux as a function of (a,c) the temperature gradient at $\chi = 0$ and (b,d) the flux surface-averaged temperature gradient $\langle \nabla \ln T \rangle$. Note : κ and δ given at reference surface $\rho = 0.5$.

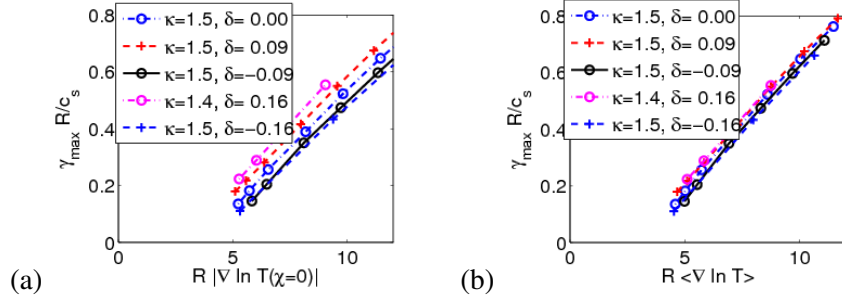


FIGURE 3. Triangularity scan at constant elongation: Same as Fig. 2 (a) and (b)

By representing the maximum growth rate of linear ITG modes as a function of either $R|\nabla \ln T(\chi = 0)| = R|\nabla x(\chi = 0)||\partial \ln T / dx|$ or $R\langle |\nabla \ln T| \rangle = R\langle |\nabla x| \rangle |\partial \ln T / dx|$, where the later can be viewed as a measure of the effective temperature gradient seen by the mode, it appears clearly that the dominant effect of elongation results from the modification of the effective spatial gradient on a given flux surface, see Fig. 2. (a) and (b). Considering both the circular and the most elongated equilibrium, nonlinear simulations are carried out and the resulting electrostatic heat fluxes have again been represented as a function of $R|\nabla \ln T(\chi = 0)|$ or $R\langle |\nabla \ln T| \rangle$, see Figs. 2. (c) and (d). By comparing Fig. 2 (b) and (d), one observes that for simulations with identical linear growth rates there remains a small difference in the nonlinear heat flux. Nonetheless these results basically confirm that the dominant effect of elongation can be explained by the modification of the effective gradient.

Concerning the effect of triangularity, preliminary results show that the modification

of the spatial gradient partly explains its effect on linear growth rates, see Fig. 3 (a) and (b). The remaining differences might arise from the modification of ∇B which is at the origin of the curvature drive. The variation of ∇B is indeed observed to be much more significant in the case of the δ scan than for the κ scan.

DEVELOPMENT OF A GLOBAL VERSION OF THE GENE CODE

In order to address the issue of non-local effects in turbulent transport, a global version of the GENE code is under development. As a first step towards this goal, the x variation of equilibrium quantities are being introduced in the flux tube gyrokinetic equation (1) and in the field equations. In view of such modifications, the original Fourier representation for the radial direction is replaced by a real space treatment. This requires to adapt the radial derivatives, which are now treated using 4th order centered finite differences, similar to the derivatives in the z direction. In addition, the Fourier space gyroaveraging operator $\bar{\Phi}(k_x, k_y, z, \mu) = J_0(k_x, k_y, z, \mu)\Phi(k_x, k_y, z)$ is replaced in the x direction by the real space gyroaveraging integral, for which a cubic-Hermite interpolation has been applied, leading to a banded matrix operator applied on ϕ . A similar treatment is used for the field solver.

Furthermore, in the Fourier version of the code, when dealing with the nonlinear term, an anti-aliasing procedure is used to avoid pollution of the spectra by unresolved modes which may even lead to numerical instabilities. A scheme has been introduced to achieve similar anti-aliasing in real space. When starting in Fourier space, the anti-aliasing procedure consists of two steps: (1) First the spectrum is extended and padded with zeros before the nonlinear multiplication is carried out in real space. (2) The extended spectrum is then removed from the nonlinear product which has been previously back-transformed in Fourier space. These two steps correspond in real space to (1) an interpolation, followed by (2) a smoothing operation. When working in real space these two operations should remain local for practical reasons. As a result, these two real space operators can only approach their Fourier space counterpart. The schemes used are a 9th order Lagrange interpolation and a ten points smoothing operator. Results in Fig. 4 are obtained with a version of the code which still uses Fourier treatment of the x derivatives and field solver, but with the real space anti-aliasing procedure. For stability reasons, a hyperdiffusion term of the form $h_x(k_x\Delta_x)^4 f$ nonetheless needed to be added to the gyrokinetic equation. The real space anti-aliasing enables one to use a lower value of the hyperdiffusion coefficient h_x required to obtain a stable simulation compared to the case where no anti-aliasing was used. In addition, the resulting k_x density spectrum is much closer to the simulations with Fourier space anti-aliasing.

CONCLUSION

In the present work, we have shown that the approximation made on the straight field line angle in the $s - \alpha$ model leads to significant differences in the linear growth rate of ITG modes for Cyclone parameters. Furthermore, true agreement can be obtained between flux tube and global codes when both use a consistent treatment of the geometry and in

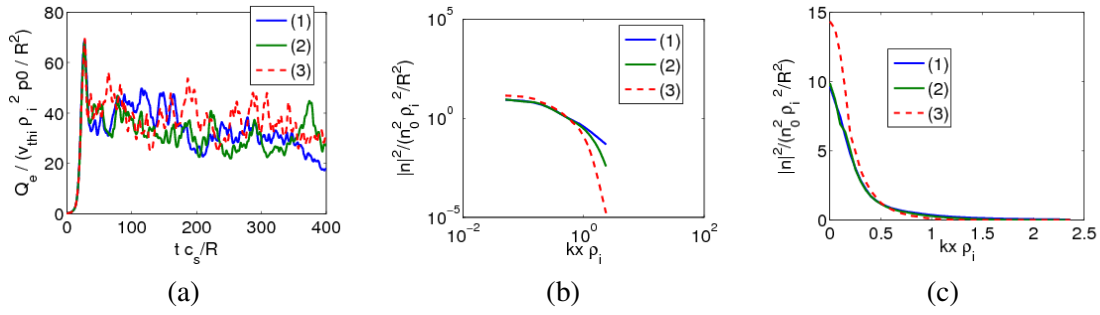


FIGURE 4. (a) Electrostatic heat flux time trace, (b) k_x density spectrum in logarithm and (c) linear scale. The different curves are obtained using (1) the standard Fourier anti-aliasing and $h_x = 0$, (2) the real space anti-aliasing with Lagrange interpolation of order 9 and $h_x = 0.6$, and (3) no anti-aliasing and $h_x = 4$.

the appropriate $\rho^* \rightarrow 0$ limit for the later. Performing simulations for different plasma shapes, it appears that the main effect of elongation on linear ITG modes results from the modification of the effective flux surface-averaged gradient. This dominant effect was essentially confirmed when considering non-linear simulations. The triangularity effect can also partly be explained by the modification of the spatial gradient, however their remains small differences which might be due to the modification of ∇B . A more detailed analysis is in progress. Finally, the present stage of the development of a global version of GENE was presented. In view of introducing radial profiles of equilibrium quantities, the treatment of the radial direction was changed from Fourier to real space, which has required to adapt the radial derivatives, the gyro-averaging and the field solver, as well as the anti-aliasing procedure used when dealing with the nonlinear term.

REFERENCES

1. F. Jenko, W. Dorland, M. Kotschenreuther, and B. N. Rogers, Phys. Plasmas **7**, 1904 (2000).
2. T. Dannert and F. Jenko, Phys. Plasmas **12**, 072309 (2005).
3. A. M. Dimits, G. Bateman, M. A. Beer, *et al.*, Phys. Plasmas **7**, 969 (2000).
4. G. Rewoldt, W. M. Tang, and M. S. Chance, Physics of Fluids **25**, 480 (1982).
5. D. D. Hua, X. Q. Xu, and T. K. Fowler, Phys. Fluids B **4**, 3216 (1992).
6. J. E. Kinsey, R. E. Waltz, and J. Candy, Physics of Plasmas **14**, 102306 (pages 13) (2007).
7. H. Lütjens, A. Bondeson, and O. Sauter, Comp. Phys. Comm. **97**, 219 (1996).
8. M. Kotschenreuther, G. Rewoldt, and W. Tang, Comp. Phys. Comm. **88**, 128 (1995).
9. W. Dorland, F. Jenko, M. Kotschenreuther, and B. N. Rogers, Phys. Rev. Lett. **85**, 5579 (2000).

ACKNOWLEDGMENT

This work was partly supported by the Swiss National Science Foundation. The simulations have been run on the Pleiades2 cluster and the IBM Blue Gene parallel machine at EPFL. The authors would like to thank O. Sauter and T. M. Tran for their help concerning the implementation of the CHEASE code interface.